



ORIGINAL ARTICLE

Daniela Addressi · Francesco D'Annibale · Luca Placidi ·
Ivan Giorgio

A bone remodeling approach encoding the effect of damage and a diffusive bio-mechanical stimulus

Received: 10 November 2023 / Accepted: 1 May 2024
© The Author(s) 2024

Abstract The paper focuses on the effect of damage on the bone remodeling process. This is a crucial, although complex, aspect. A one-dimensional continuous deformable body is employed to model living bone tissue. The model incorporates the bone functional adaptation through an evolution law for an effective elastic modulus driven by mechanical feedback via a mechano-transduction diffusive signal. This type of information transduction, i.e., diffusion, is essential for the model to take into account remodeling in the case of minor injury or pathology-affected regions where there is no signal production. In addition, the model is able to also take into account potential tissue damage that may evolve over time according to a suitable evolution law. To illustrate the capability of the model to describe the mentioned complex coupled phenomena, numerical tests have been performed encompassing high external loads causing the onset of damage and cyclic loading for healing. The numerical simulations carried out via finite-element analyses yield insights into the mechanisms of bone remodeling, with the final goal of aiding clinical decisions and implant designs for bone health and repair. Overall, a key aspect of the paper is to highlight the feasibility of modeling the evolution in bone elasticity arising from the combined effect of damage and remodeling.

Keywords Bone remodeling · Mechanical stimulus · Damage · Finite element method

Francesco D'Annibale, Luca Placidi and Ivan Giorgio have contributed equally.

D. Addressi
Department of Structural and Geotechnical Engineering (DISG), Sapienza University of Rome, 18, Via Eudossiana, 00184 Rome, Italy
E-mail: daniela.addressi@uniroma1.it

F. D'Annibale · I. Giorgio (✉)
Department of Civil, Construction-Architectural and Environmental Engineering (DICEAA), University of L'Aquila, 1, P.zza Ernesto Pontieri, Monteluco di Roio, 67100 L'Aquila, Italy
E-mail: ivan.giorgio@univaq.it

F. D'Annibale
E-mail: francesco.dannibale@univaq.it

L. Placidi
Engineering Faculty, International Telematic University Uninettuno, 39, Corso Vittorio Emanuele II, 00186 Rome, Italy
E-mail: luca.placidi@uninettunouniversity.net

F. D'Annibale · L. Placidi · I. Giorgio
International Research Center for the Mathematics and Mechanics of Complex Systems (M&MoCS), University of L'Aquila, 1, P.zza Ernesto Pontieri, Monteluco di Roio, 67100 L'Aquila, Italy

1 Introduction

The primary functions of the bone are to sustain the body weight, provide leverage for motion, and protect vital organs. Therefore, its principal purpose is of a mechanical nature. The remodeling process is a biological process that has evolved over millions of years for vertebrates to ensure that the skeleton is optimized for functionality and longevity. Indeed, the mechanical strength of the bone tissue continuously adapts itself to the mechanical demands of the environment, saving as many resources (oxygen, nutrients, and energy) as possible to improve the efficiency of the bone tissue. In addition, a constant mass turnover is carried on to have some kind of 'routine maintenance' that restores micro-cracked tissue with newly produced tissue.

Bone remodeling is a crucial physiological process that ensures the continuous adaptation and maintenance of bone tissue in response to mechanical loads and external stimuli [1–3]. A deep knowledge of the intricate mechanisms involved in bone remodeling is essential to developing effective treatments for bone-related diseases and optimizing implant designs.

To be noted is that, in this framework, damage plays a crucial role in bone remodeling for several reasons:

1. *Natural wear and tear*: Bones are subjected to constant mechanical stresses in daily life. Over time, micro-damage accumulates due to activities like walking, running, and lifting. Understanding how this accumulated damage affects bone health is essential.
2. *Injury response*: When bones are subjected to trauma or fractures, they undergo a healing process. This healing involves the removal of damaged bone tissue and the formation of new bone. Damage considerations are vital in predicting how well bones will heal and regain their original strength.
3. *Pathologies*: Specific medical conditions and diseases can lead to bone damage. For example, osteoporosis causes bones to become brittle and prone to fractures. Incorporating damage into bone remodeling models helps in understanding disease progression and potential treatments.
4. *Clinical interventions*: Surgeons and healthcare professionals often need to assess the impact of surgeries or implantations on bone health. Models that account for damage are essential in predicting how bones will respond to these surgeries.
5. *Optimizing implant designs*: When designing implants or prosthetics that interact with bone, it is crucial to consider how they might affect the surrounding bone tissue. Damage modeling helps in optimizing implant designs for long-term compatibility and reducing the risk of complications.
6. *Long-term bone health*: The accumulation of damage in bones can lead to conditions like stress fractures or chronic pain. Understanding how damage affects the long-term health of bones is vital for preventing these issues.
7. *Tailored therapies*: Damage-informed models can aid in developing personalized therapies for individuals with bone-related conditions. By predicting how a person's bones respond to damage and healing, treatments can be optimized for better outcomes.

Then, it appears to be quite evident that incorporating damage phenomena into bone remodeling models is crucial to comprehensively understanding bone health and addressing a wide range of clinical, biomechanical, and healthcare challenges. It helps in predicting bone behavior under various conditions, from everyday activities to traumatic injuries, ultimately contributing to better patient care and medical advancements.

Some models related to damage in bone remodeling have already been conceived in the literature [4–6]. These models delved into the micro-level of observation to understand the mechanisms that may be involved in the influence of damage on remodeling. However, there are only a few attempts being made to address the damage modeling at a macroscopic scale (see, e.g., [7, 8], which considers damage based on fatigue). For some more details about damage in the continuum framework, see [9–17]. Really, the overall effect of damage on bones is quite complex since it involves not only loss of strength in the bone but also hypoxia due to the rupture of blood vessels that cannot work correctly. This lack of a vascular network causes living cells to deplete necessary nutrients, leading to undernourished cells expressing signals of nutrient demand. Some models that address these aspects have been proposed [18–20], but here, we refrain from considering this aspect for the sake of simplicity and tractability.

The primary cause of bone remodeling is mechanical loading. When bones experience mechanical forces, such as weight-bearing activities or muscle contractions, it triggers a complex series of events, such as the production and release of signaling molecules, that ultimately lead to bone remodeling. This mechanical stimulus is essential for maintaining bone strength and integrity. Particularly, when such mechanical signals are sensed by bone cells (osteocytes) and converted into biochemical signals (mechano-transduction), they regulate bone remodeling by reaching and activating other bone cells (osteoblasts and osteoclasts) in charge of the adaptive process [21]. Different models involving a variable, usually called stimulus, have been proposed

to describe the pathways of the transmission of the biochemical factors. In the first versions, a weight function depending on the distance between the different cells was introduced to take into account the exchange of information [22]. An improved version was proposed, considering a space convolution integral (firstly by [23] and then [24,25]). Recently, this concept has been further developed using the diffusion equation [26], and, therefore, in this paper, we adopt this last approach to describe the evolution of the stimulus that seems to be the most appropriate way to address the problem. It is noteworthy to state that, however, in our model, we focus on the cellular activity responsible for remodeling rather than on the evolution of cell populations and their motility. Among the models related to these aspects, we can recall [27–29].

Different aspects of living bone tissues become apparent or relevant at different time scales. A complete description of their evolution involves processes or dynamics that unfold and change over time, and these changes are noticeable and significant at various time scales. Bone dynamics, in fact, involves multiple time scales, which can range from short intervals (seconds, minutes), like the mechanical response due to the application of an external force, to much longer ones (days, weeks) related to the remodeling process. Understanding and studying time multiscale processes such as the comprehensive evolution of the bone can be challenging because one needs to consider the interactions and dependencies across different time scales. For this reason, a detailed model able to encompass all these features is still missing. The available models focus on a sole time scale to examine and predict specific aspects of the bone system. In this paper, we fall into this category of simplified approaches and investigate specifically the slow time scale associated with the remodeling.

The bone remodeling model used in this study is based on a one-dimensional (1D) continuum formulation, including both mechanical and biological factors [23]. The model accounts for the production of new solid tissue and the resorption of old and damaged tissue originating from the mechanical environment. The evolution of the mass density directly affects the elastic modulus of the bone material and, consequently, its mechanical response. Since the complexity of the phenomenon examined, the paper is intended as a preliminary step toward the development of a more comprehensive and realistic representation of bone remodeling. To this end, we also aim herein to develop a model facilitating theory-driven experiments for testing hypotheses, guiding research questions, selecting variables, and interpreting results within the context of the underlying theory.

The plan of the paper is arranged as follows. In Sect. 2, the governing equations for mechanical deformation and biological processes are coupled to simulate the evolution of a 1D bone tissue over time at the chosen time scale. We, therefore, employ a computational model implemented in COMSOL Multiphysics, in Sect. 3, to investigate the bone remodeling phenomenon under two distinct scenarios: (1) dynamic loading-induced damage in Subsect. 3.1 and (2) cyclic loading-induced healing process in Subsect. 3.2. The results of the simulations appear to be promising and, therefore, require further investigation regarding the influence of damage in the remodeling process.

2 Problem formulation

In the hypothesis of the quasi-static regime, the equation of motion for a one-dimensional (1D) bar of initial length L , expressed in terms of the axial displacement field $u(x, t)$ according to the displacement-based approach is given by:

$$\begin{cases} -[k_a(x, t) u'(x, t)]' = b(x, t) & \forall x \in [0, L], \forall t \geq 0 \\ u(0, t) = 0 & \forall t \geq 0 \\ k_a u'(L, t) = f(t) & \forall t \geq 0 \end{cases} \quad (1)$$

where the second and third equations show the essential and natural boundary conditions adopted for the bar. Here, the boundary conditions refer to a fixed left-hand side ($x = 0$) and to the application of a force f to the other ($x = L$). $k_a(x, t) = E(x, t)A(x)$ is the axial stiffness, with $E(x, t)$ denoting the actual Young's modulus, and $A(x)$ the cross-section area. The term $b(x, t)$ is a force distributed along the bar axis line work-conjugate to the displacement $u(x, t)$. In a practical scenario, b can be identified with the weight for a vertical one-dimensional body and evaluated as $\varrho_L g$ where $\varrho_L = \varrho A$ is the mass density per unit line, ϱ the apparent mass density per unit volume (we remark that bone tissue is a porous material), and g the gravity acceleration.

In the case of remodeling, we can assume that the Young modulus can evolve depending on the load applied to the bar. In particular, we can suppose that one evolution is linked to the functional adaptation of bone, as well as to possibly healing capability, while the other is related to the damage process occurring when the applied load exceeds a critical value. To keep track of these two possibilities, we introduce a representation

of Young's modulus in terms of two variables: 1) a damage accumulation β (ranging from 0 to 1); and 2) an adaptive variable γ (ranging from 0 to 1) that takes into account the change in porosity of the bone with the remodeling. Accordingly, we set the following equation:

$$E(x, t) = [1 - \beta(x, t)] \gamma(x, t) E_{\text{Max}} \quad (2)$$

where E_{Max} is the Young modulus of the solid mineral part of the bone here assumed as constant. The physical interpretation for β is similar to the classical in damage mechanics. The difference is that standard damage formulation accounts only for a passive response, no healing is accepted and β is assumed *ab initio* to be a non-decreasing function of time. Here, this assumption is removed and the healing capacity of the material is taken into account. To better explain the role of γ , we must consider that bone is a porous material, and thus γE_{Max} can be assumed as an apparent Young's modulus; hence, γ can be identified as a scaling factor for Young's modulus when no damage accumulation ($\beta = 0$) is present and associated with a certain amount of porosity with a non-prescribed, albeit intuitively monotonic, function. Besides, zero porosity corresponds to $\gamma = 1$ and unit porosity to $\gamma = 0$. During bone remodeling, synthesis or resorption of bone tissue implies just a change in the porosity of the material because of the mass change induced by such a process. Eventually, γ accounts for this mass variation and, in turn, that of the porosity affecting the modification of Young's modulus. For more information on the microscopic phenomena underlying Eq. (2) and the mechanical-biological aspects of the proposed model, we recommend consulting the sources [30–32]. To summarize, the proposed model is characterized by two microstructures: one that represents the healthy state of bone tissue, primarily related to the various types of porosities (intertrabecular, vascular, lacunar-canalicular, collagen-apatite related) and the other that represents damage accumulation, mainly consisting of micro-cracks. The evolution of these microstructures is influenced by two factors: excessive mechanical loads that are applied and bone remodeling through the breakdown of old tissue, which can be potentially affected by microcracks, and the formation of new tissue with mechanical strength dictated by the level of external forces applied to the bone. Therefore, we distinguish the evolution of these two microstructures, as microcracks can only be generated by the application of external forces. On the other hand, the biological activities of bone cells affect the evolution of both microstructures. They cure the possible damage present and increase or decrease the stiffness and strength of the bone tissue depending on the level of deformation that is determined within the bone.

In view of the above definitions, we can postulate a remodeling law for the “healthy” part ($\gamma(x, t) E_{\text{Max}}$) of Young's modulus as follows [33]:

$$d_\gamma \frac{\partial \gamma}{\partial t} = \mathcal{A}(S) H(\gamma) \quad (3)$$

where the function $\mathcal{A}(S)$ drives the evolution of γ based on the mechanical state of the system given by the stimulus S (to be later defined), and d_γ is a growth and decay parameter that specifies the characteristic time of such evolution. To simplify the notation from this point on, we omit the dependence on space and time except in cases where it may cause misunderstandings. On the one hand, the function H represents a weight that hinders the process when γ goes towards its limits, namely 0 and 1, corresponding, as already remarked, to 1 and 0 porosity, respectively. These circumstances are well-known to impede bone remodeling in these extreme cases (see Eq. (4) and the conditions $H(0) = H(1) = 0$). The reason is that the bone cells in charge of the process need both support over which they can lay and some room to operate within the bone pores. The function H takes into account the inner surface of the pores, and the most simple version of it can be specified as:

$$H(\gamma) = \begin{cases} 4\gamma(1-\gamma) & 0 \leq \gamma \leq 1 \\ 0 & \gamma < 0 \wedge \gamma > 1 \end{cases} \quad (4)$$

that corresponds to an arbitrary optimal value for the adaptive variable $\gamma = \gamma_{\text{opt}} = 0.5$ that can be changed according to the experiments. It is worth noting that here we choose this shape for H for the sake of simplicity, but this function can also be the object of an experimental identification (see, for more details, [34]).

On the other hand, a simple trend for $\mathcal{A}(S)$ that considers the homeostatic state of the bone is given by the piece-wise linear function:

$$\mathcal{A}(S) = \begin{cases} r_s(S - S_s) & S - S_s \geq 0 \\ 0 & S_r \leq S \leq S_s \\ r_r(S - S_r) & S - S_r \leq 0 \end{cases} \quad (5)$$

where S_r and S_s are two thresholds that define a region of homeostasis. The parameters r_s and r_r are two constitutive coefficients representing the influence of the stimulus S on the rate for the synthesis and resorption of bone material, respectively.

The stimulus S carries on the information related to the mechanical state of the bone and can be introduced in the model through the following diffusion equation:

$$\begin{cases} d_S \frac{\partial S}{\partial t} = (\kappa S')' + r(U) - s(S) & \forall x \in [0, L], \forall t \geq 0 \\ S'(0, t) = S'(L, t) = 0 & \forall t \geq 0 \\ S(x, 0) = S_0 & \forall x \in [0, L] \end{cases} \quad (6)$$

where the coefficient κ is a diffusion parameter, d_S is a constant representing the characteristic time of the diffusion phenomenon, r is a source term, and s is a sink term. The initial value for S is assumed to be at equilibrium in the homeostatic state; thus, we set it to be $S_0 = (S_s + S_r)/2$, for the sake of simplicity. In terms of boundary conditions, we implemented a Neumann boundary condition that reflects zero stimulus flux. This was applied to simulate an isolated scenario where external factors do not influence the specimen. Specifically, the source is assumed to be proportional to the strain energy density U as follows:

$$r(U) = g_S U = g_S \frac{1}{2} k_a(x, t) (u')^2 \quad (7)$$

where the constant of proportionality g_S can be interpreted as a gain on the detected signal. As further developments, other possibilities could be conceived; for example, possibly a direct dependence for the stimulus evolution upon the damage β or dissipation energy, following some alternative concepts explored in literature [35]. Here, we prefer to keep the model as simple as possible to have a more profound comprehension of some aspects of the remodeling process that we have already incorporated into the model. The sink is defined as linear in the stimulus starting from an activation threshold \bar{S} . Here, we set $\bar{S} = S_s$ and introduce R as the non-dimensional proportionality coefficient, as:

$$s(S) = \begin{cases} R(S - \bar{S}) & S - \bar{S} \geq 0 \\ 0 & S - \bar{S} < 0 \end{cases} \quad (8)$$

Naturally, if the stimulus is absent ($S = 0$) or lower than a set threshold ($S < \bar{S} = S_s$), then no resorption occurs.

In the context of bone remodeling, a stimulus often refers to any factor or influence that triggers the process of bone resorption and formation. Stimuli can include various factors such as mechanical loading (physical activity), hormonal influences (such as parathyroid hormone and calcitonin), and systemic factors (like calcium and vitamin D levels). The most well-understood stimulus for bone remodeling is the mechanical one caused by weight-bearing exercise and muscle contractions. During physical activities, specific cells (osteocytes) sense and transduce the mechanical sources of stimulation and synthesize local paracrine factors (chemical messengers involved in cell communication) that induce changes in neighboring cells (osteoblasts and osteoclasts) to regulate bone remodeling, thus leading to the breakdown and formation of bone tissue, and ultimately maintaining bone integrity and functionality. Overall, bone remodeling is a complex biological process that is governed by the interplay between bone cells and the mechanical loadings placed on them. The mechanical loadings determine the environment where the cells reside and, in turn, influence their behavior through feedback mechanisms. This intricate interplay between biological and mechanical factors is crucial in maintaining the integrity and strength of bones. At this preliminary stage, we refrain from any effort directed to have a complete and simultaneous description of all the phenomena occurring in the bone remodeling process, especially those biologically related to the micro-description of the stimulus, since this may lead to models too complex to be treatable. However, to provide a brief synoptic view of how bone cells behave during the process of remodeling, we can refer to studies where bone cells were exposed to fluid flow or pulsating hydrostatic pressure [36]. It has been shown that pulsating hydrostatic pressure is relevant under standard physiological loading conditions [37]. The changes in hydrostatic pressure at the observation scales of vascular or lacunar pores, as discussed in [27], are accompanied by changes in strain energy density at the extravascular scale [38,39]. This provides a microstructural and micromechanical basis for using U as a source of mechanical stimulus. Here, we attempt to conceive a macroscopic synthetic description with a suitable compromise between the capability of predicting the phenomena and manageability. In this spirit, the

source term $r(U)$ in Eq. (6) takes account of the mechanical stimulation through the strain energy density U , while the introduced variable S more specifically can be identified with the level or the concentration of paracrine factors originating in the signaling pathways involved in the process initiated by that mechanical source term. Therefore, we assume $S \geq 0$.

Finally, we can assume an evolution law for the damage as follows:

$$d_\beta \frac{\partial \beta}{\partial t} = \varphi(u') (e^{-\varsigma \beta} - e^{-\varsigma}) - \mathcal{B}(S - S_s) H(\beta) \quad (9)$$

where we underline two competitive actions, one due to the positive function φ , which is a damaging action that defines a yield criterion for the bone and depends on the deformation u' , while \mathcal{B} represents the healing capability of the material and can be thought of as a linear function of the stimulus. The exponential weight function in Eq. (9) is introduced to slow down damage evolution when β tends to 1 in order to avoid values of β greater than 1. The coefficient ς is a positive coefficient to be identified via experiments. The function H (defined in Eq. (4), being here β the argument) implies that the healing process occurs only when damage accumulation is in a proper range and it is zero both for $\beta = 0$ and $\beta = 1$, because, of course, there is no need for healing if there is no damage accumulation. It is worth noting here that again, the function H is conceived to have an optimal value of damage $\beta = \beta_{opt} = 0.5$ that should be better calibrated with experiments.

We remark that despite the similar role of \mathcal{A} in Eq. (3) and \mathcal{B} in Eq. (9), indeed, they represent a source contribution providing new bone tissue; there is a decisive difference in their outcome that urges us to differentiate their effects and place them in the equations mentioned above to better mimic the phenomenology of the remodeling process in the presence of damage. On the one hand, the action of \mathcal{A} is related to a change in the porosity level of the bone tissue originating from the mechanical stimulation, both increasing and decreasing the amount of the porous volume (affects γ). On the other hand, the effect of \mathcal{B} is only oriented to heal possible micro-cracks produced by the damage accumulation and, therefore, solely affects the variable β , decreasing it. Naturally, the two actions must be well-calibrated to avoid forcing β and γ outside their definition range.

The parameter d_β is the characteristic time for damage evolution. Besides, we assumed for φ a bathtub curve as follows:

$$\varphi(u') = \begin{cases} \Phi_\ell & u' < -(V_c + u'_c) \\ \Phi_\ell \left[3 \left(\frac{-u' - u'_c}{V_c} \right)^2 - 2 \left(\frac{-u' - u'_c}{V_c} \right)^3 \right] & -(V_c + u'_c) \leq u' \leq -u'_c \\ 0 & -u'_c < u' < u'_s \\ \Phi_\ell \left[3 \left(\frac{u' - u'_s}{V_s} \right)^2 - 2 \left(\frac{u' - u'_s}{V_s} \right)^3 \right] & u'_s \leq u' \leq V_s + u'_s \\ \Phi_\ell & u' > V_s + u'_s \end{cases} \quad (10)$$

where V_c , V_s , u'_c , u'_s , and Φ_ℓ are parameters that can be used to define the yield points and the rate of evolution associated with the damage variable.

Regarding the healing function \mathcal{B} , we set:

$$\mathcal{B}(S) = \begin{cases} r_s(S - S_s) & S - S_s \geq 0 \\ 0 & S - S_s < 0 \end{cases} \quad (11)$$

3 Numerical simulations and discussions

To demonstrate the versatility of the simple model introduced in the previous section, we now examine pivotal aspects of the model through a numerical study of the aforementioned one-dimensional bone bar in some significant scenarios. Therefore, the previously introduced governing equations are solved with the finite element method implemented with a weak formulation in the commercial software Comsol multiphysics. The material parameters that establish the required link between mechanical and biological phenomena are set as reported in Table 1. It is worth noting that the model is rate-dependent via the characteristic times d_S , d_β , and d_γ . These quantities have been presented in Table 1 in a generic unit of time that can be chosen with experiments as week, month, years, etc., according to the investigated problem.

We conduct a parametric study for two paradigmatic cases: (1) loading-induced damage and (2) cyclic loading-induced healing process with initial damage. We vary parameters such as the biological and mechanical

Table 1 Constituent parameters that we used in the numerical analysis

r_s	r_r	S_s	S_r	E_{Max}	ζ
1 N^{-1}	3 N^{-1}	0.035 N	0.013 N	18 GPa	1
g_S	R	d_S	d_β	Φ_ℓ	d_γ
0.1	13	1 UT	0.05 UT	10	80 UT
κ	V_c	V_s	u'_c	u'_s	\bar{S}
1 m^2	0.04	0.04	0.02	0.02	0.035 N

evolution coefficients, the loading magnitude, and the loading frequency. By systematically changing these parameters, we gain insights into the sensitivity of the bone remodeling response to different factors.

In the following numerical study, a cylindrical bone sample with a length L of 10cm and a radius r of 0.5 cm is considered in such a way that $A(x) = \pi r^2 = \pi/4 \text{ cm}^2$. The Young modulus of the solid mineral part E_{Max} is set, according to Table 1, to be 18 GPa, the mass density ρ is 1800 kg/m^3 .

3.1 Case of a significant external force causing damage

In the first case, we simulate a rod made of bone subjected to a loading event variable over time. The rod is subjected to a force of sufficient magnitude to induce damage. The objectives of this case are to examine the interplay between the healing process and the evolution of the damage during the numerical experiments and predict the subsequent remodeling response. The loading, modeled with a Gaussian time history for the sake of simplicity and tractability, is applied over a limited interval of time to replicate a repeated circumstance that induces damage after a prolonged interval of time. In the proposed model, indeed, a sudden external impact cannot be considered because it happens at a time scale very fast with respect to the scale of the remodeling process. For the sake of simplicity, we take into consideration only the time scale compatible with bone remodeling. All the forces applied must be assumed as effective or equivalent quantities that introduce the same amount of energy as the instantaneous forces in the system [40].

Particularly, we apply the external force

$$f(t) = F_h + F_0 e^{-\frac{1}{2} \left(\frac{t-t_d}{\Delta_t} \right)^2} \quad (12)$$

where a constant value of the magnitude, $F_h = 214.3 \text{ N}$, is considered to maintain the homeostasis state (this value corresponds to a deformation of around $1000 \mu\text{strain}$, which is commonly associated with the homeostatic state [41]), while the peak value due to $F_0 = 64.29 \times 10^3 \text{ N}$ is conceived to initialize damage within the specimen. Besides, we set the instant of the maximum peak of the damage-inducing load to $t_d = 0.3 \text{ UT}$ (unit of time, which is set to be one week in our problem) and the extent of the time interval over which this load is spread out to $\Delta_t = 0.0316 \text{ UT}$.

We chose to vary some parameters that describe the amplitude of the exciting force F_0 , the stimulus evolution, g_S , R , and d_S , the damage accumulation, d_β and Φ_ℓ , and the evolution of γ , d_γ for parametric analyses. These parameters are distinctive of the proposed model, while other parameters, such as the synthesis or resorption rates, have been left unchanged since their influence is easily predictable. For this case, we show, as a result of the simulations, three panels illustrating the main variables associated with the evolution of the bone tissue: the damage accumulation β , the normalized Young modulus in the absence of damage γ , and the comprehensive normalized elastic modulus $(1 - \beta) \gamma$. In this way, we can analyze the damage evolution and the healing process separately and examine their combined action.

Figure 1 shows the influence of the amplitude of the force F_0 varying in the range $(0.4 - 1.4) F_0$. We observe that low values of this parameter delay the onset of damage, which does not propagate because the force is soon removed. This delay causes less stimulus to be produced; thus, the value of γ remains almost unchanged. As the magnitude of the excitatory force increases, the damage anticipates its onset, and this promotes more deformation for longer and, thus, more stimulus, which heals the damage and raises, albeit slightly in the example considered, the increase in γ .

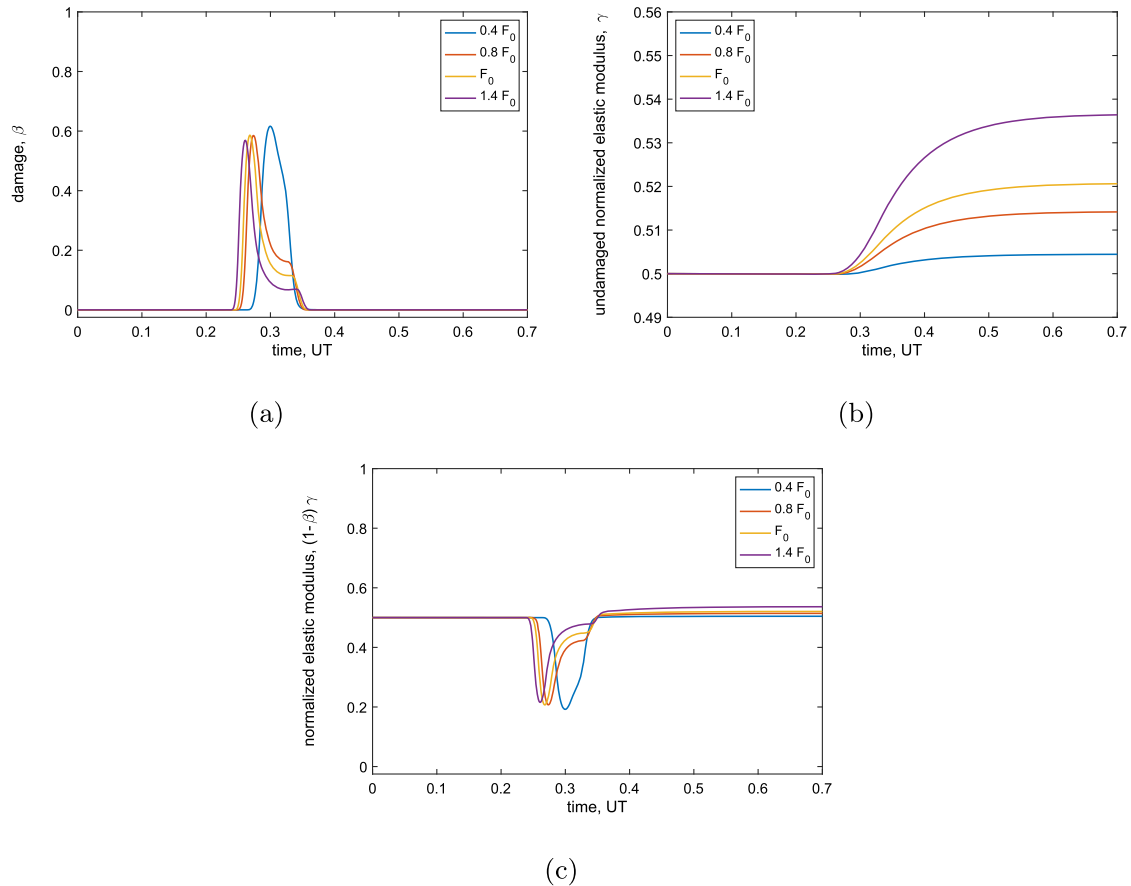


Fig. 1 Effect of the parameter F_0 on damage (a), undamaged normalized elastic modulus (b), and normalized elastic modulus (c)

Figure 2 shows the influence of the parameter g_S associated with the production of the stimulus. In the plots, the time is measured in UT (unit of time, namely, one week). The reference value of g_S can be tuned in order to modulate the magnitude of the stimulus and benefit or hinder its production. In this paper, we set this value to 0.1 to obtain a plausible outcome of the amount of stimulus and, consequently, of the production of new bone. Besides, the range of parametric sweep is (0.1–10) g_S . For small values of g_S , the obtained stimulus remains low, and consequently, the healing process. On the contrary, the damage persists for a more extended period of time. As the values of g_S increase, these trends reverse, inhibiting almost completely the damage for the highest values and promoting the growth of γ that remains higher than the initial value after the removal of the excess force causing the damage. In fact, once produced, the stimulus persists for a while and then undergoes gradual resorption.

In Fig. 3, we can examine the effect of the R parameter related to the stimulus resorption cycle for normal metabolic activities. Its reference value is assumed to be 13, and the range of parametric sweep is (0.1–5) R . It represents the rate of stimulus reabsorption; therefore, low values of R imply a more remarkable persistence of the stimulus originated by the external mechanical load. This results in significant growth of γ and a greater impact on damage that is hindered. In contrast, high values of R induce a poor presence of the stimulus that is very rapidly metabolized. The healing effect is reduced, and above a certain level of R , the damage induced by the external mechanical interaction is not fully recovered.

It is worth noting that the characteristic times related to the evolution of the stimulus, the damage, and γ are different since these three phenomena actually occur at a distinct pace [42–46]. Therefore, we selected the ratios of the reference values of the parameters d_S , d_β , and d_γ in order to take into account these differences. In fact, we can assume that the fastest phenomenon is related to the damage, the slowest to the remodeling process involving γ , while for the stimulus, an intermediate rate of evolution fits with the knowledge we have so far on the overall process.

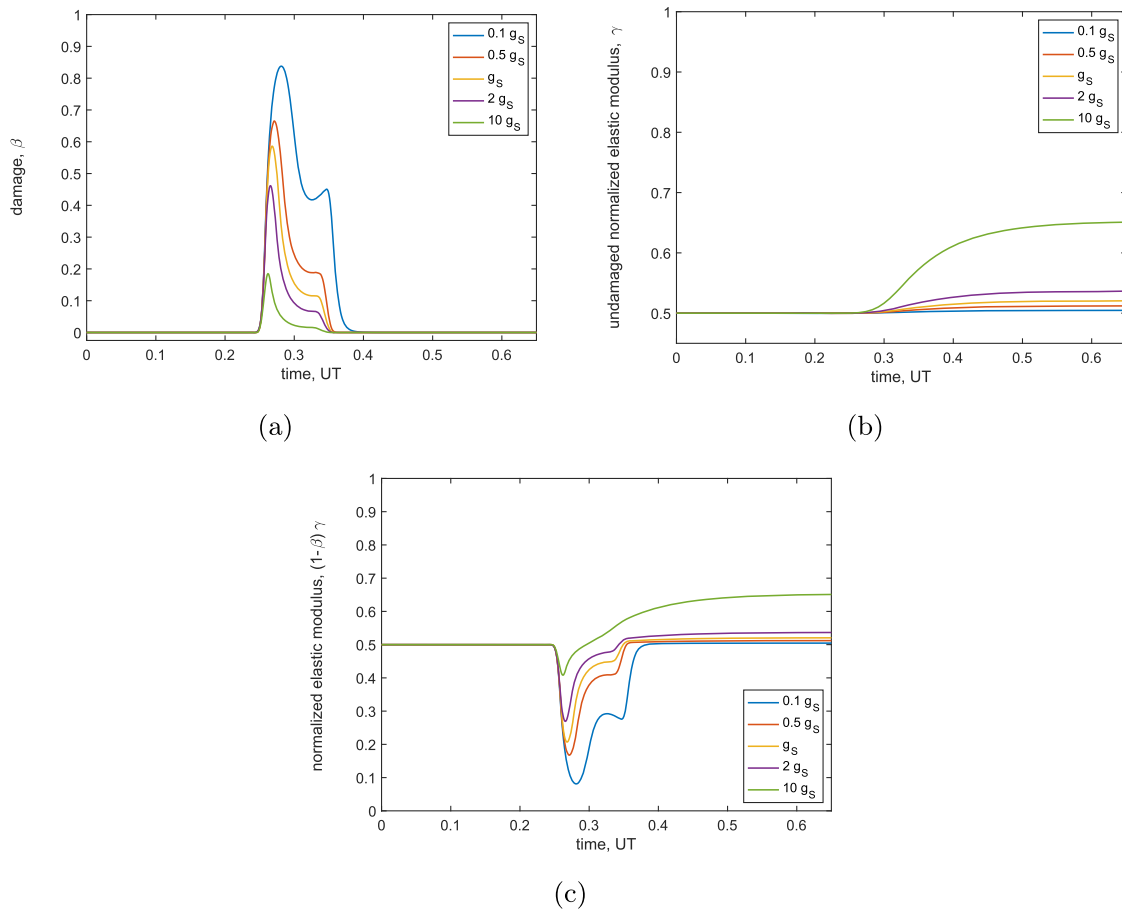


Fig. 2 Effect of the parameter g_S on damage (a), undamaged normalized elastic modulus (b), and normalized elastic modulus (c)

Figure 4 illustrates the effect of the d_S parameter affecting the characteristic time of the diffusion process associated with the stimulus. The assumed reference value is 1 UT, and the range of parametric sweep is $(0.1-20)d_S$. Low values of this parameter induce very rapid stimulus dynamics by localizing its effect in time. The damage is cured very quickly, and the residual effect of the healing process remains barely perceptible, with a value of γ just above the initial one. In contrast, high values of d_S slow down the stimulus dynamics, promoting an extension of the damage that is healed less quickly and simultaneously resulting in a stiffer final bone since the resorption of the stimulus is also slowed.

The influence of the parameter d_β is shown in Fig. 5. This parameter is associated with the characteristic time of damage evolution. In fact, from the figure, almost no relevance of it is perceived in the process of growth and resorption of the modulus γ . The reference value is assumed to be 0.05 UT, and the range of parametric sweep is $(0.1-10)d_\beta$. It, on the other hand, has a significant effect on damage progression. Small values induce a higher rate of damage caused by a more rapid response to external forcing. Therefore, as this parameter increases, the damage propensity decreases because the corresponding dynamics becomes slower. Thus, we observe less damage for high values of d_β since the load-inducing it has already been removed by the time the damage starts to emerge.

The influence of the parameter Φ_ℓ is summarized in Fig. 6. We assume that the value of reference used for Φ_ℓ is 10, and the range of parametric sweep is $(0.1-5)\Phi_\ell$. Here, a minor contribution can be detected in the evolution of the modulus γ for its growth or resorption processes; however, it is a bit larger than what occurs for d_β . Like d_β , Φ_ℓ significantly affects damage evolution, but this time, small values result in smaller damage while, increasing it, the damage accumulated grows as well. We can note that the more significant damage obtained for high values of Φ_ℓ corresponds to a slightly greater residual value of γ . This effect can

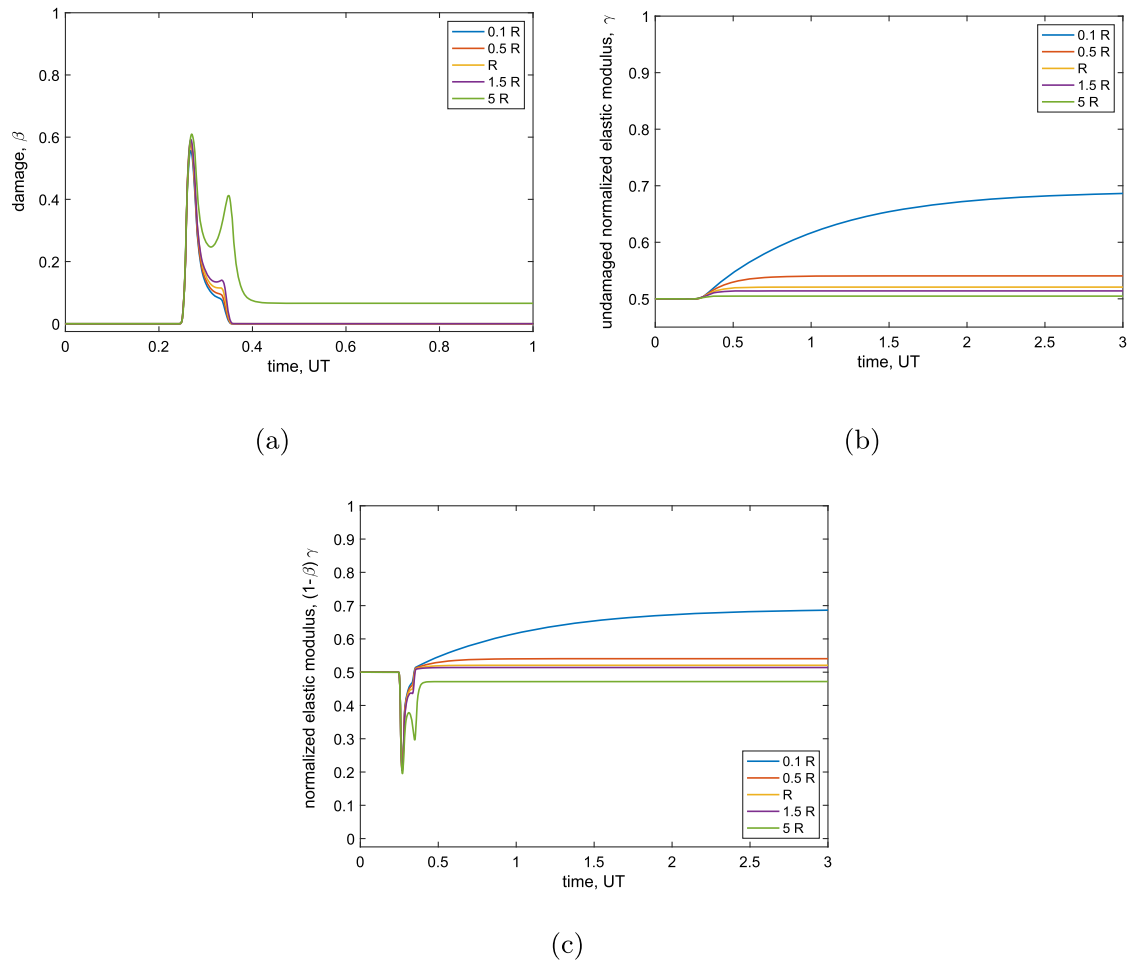


Fig. 3 Effect of the parameter R on damage (a), undamaged normalized elastic modulus (b), and normalized elastic modulus (c)

be explained by considering that high damage implies a larger deformation and, consequently, a higher level of stimulus, which is beneficial for the growth of the tissue and, in turn, for its stiffness.

The influence of the parameter d_γ is exhibited in Fig. 7. The assumed reference value of d_γ is 80 UT, and the range of parametric sweep is $(0.05-10)d_\gamma$. As we can expect, the effect of the parameter d_γ does not influence the evolution of the damage. On the contrary, it is decisive for the evolution of the elastic modulus γ . The smaller its value, the greater the resulting value of the module γ will be at the end of the numerical experiment. Indeed, the system response relative to γ is faster when its value is lower. If it has high values instead, these induce substantially no evolution of γ .

3.2 Case of an initial damaged zone with a periodic healing force for rehabilitation

In the second case, we explore the healing process associated with cyclic loading. The bone rod is assumed to have an initial level of damage localized in a chosen region, namely,

$$\beta_0 = 0.5 e^{-\frac{1}{2} \left(\frac{x-x_0}{\Delta_x} \right)^2} \quad (13)$$

where $x_0 = 0.3L$ and $\Delta_x = 0.0707L$.

A cyclic external force, modeled as a sinusoidal load, is applied to the sample to stimulate the healing process. In detail, we apply the external force

$$f(t) = F_h + F_0 \sin(2\pi f_h t) \quad (14)$$

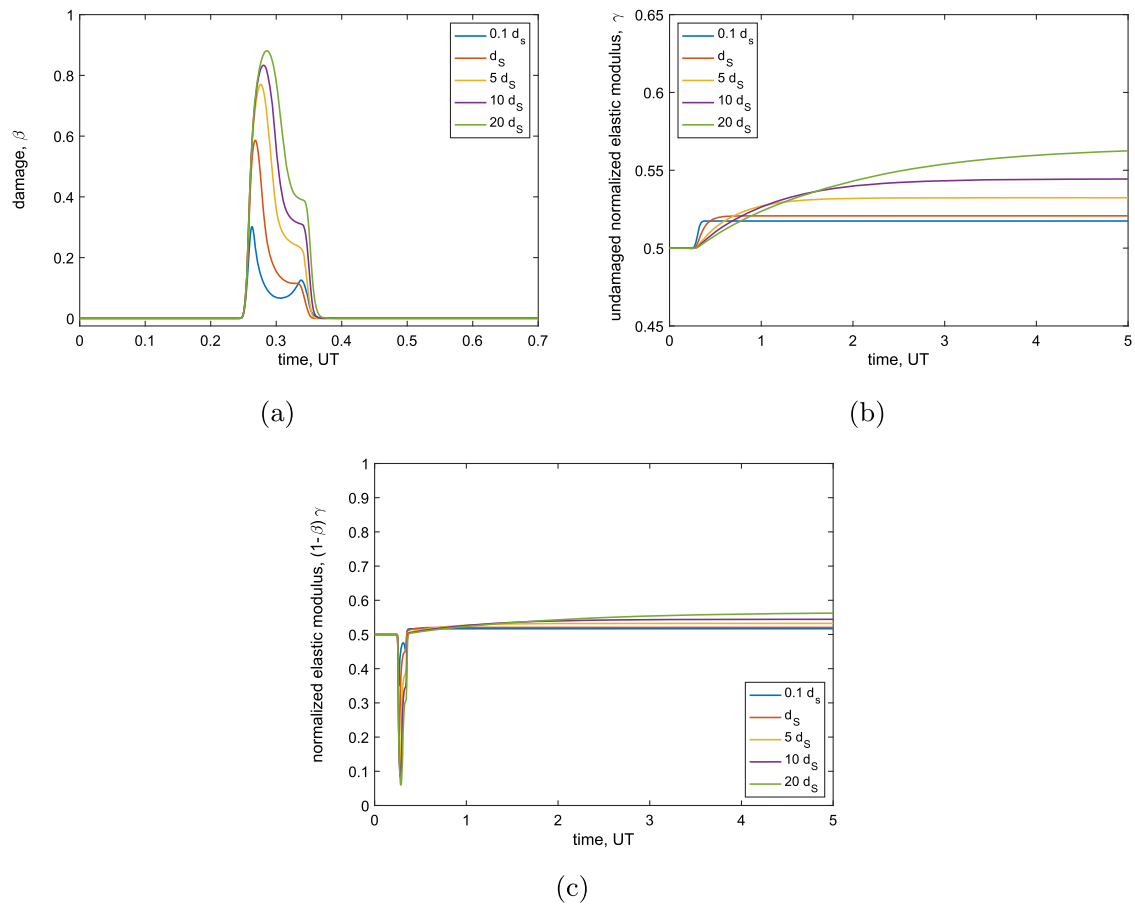


Fig. 4 Effect of the parameter d_S on damage (a), undamaged normalized elastic modulus (b), and normalized elastic modulus (c)

F_h being the same as in the previous case and modulating, in the numerical analysis, the amplitude F_0 and frequency f_h of the sinusoidally varying contribution. The low magnitude F_0 of the cyclic force ensures that the loading remains within the elastic regime of the bone. Our aim, in this case, is to track the healing progression over multiple loading cycles and investigate how the bone tissue adapts and repairs itself under cyclic loading.

In the first test performed, we see how the effect of the added cyclic force promotes the process of healing and restoration of healthy conditions. Figure 8, which shows the profile of the overall elastic modulus on the analyzed bone sample at different time instants, shows how the initial loss of stiffness due to damage is gradually recovered until complete restoration. Figure 9, on the other hand, shows the time history of the damage, the elastic modulus γ , and the total modulus at the point corresponding to the initial maximum damage, i.e., x_0 . As can be seen from the figure, the low value of F_0 implies a substantial absence of γ evolution, while the damage progressively decreases at a specific rate until it disappears altogether. In the simulation, we set $F_0 = 6.43 \times 10^3$ N and $f_h = 1$ UT⁻¹.

Afterward, we varied the loading frequency, decreasing and increasing it by ten times, to investigate its influence. Figures 10 and 11 show the time histories of damage and elastic moduli at the point of initial maximum damage, as done in the previous case, for the decrease in frequency and its increase, respectively. The qualitative trend remains the same as in the reference case. However, in these simulations and both cases, there is a decrease in velocity, more pronounced in the low-frequency case. The spatial evolution is almost the same as in Fig. 8, so it has not been reported for the sake of brevity. This frequency dependence is quite remarkable since it suggests the presence of at least a local optimal frequency for which the restoration rate of damage-free conditions is maximal. In our case, this circumstance is close to the reference frequency we have chosen. This aspect agrees with experimental observations [47–50]; therefore, it is essential. This feature is absent in previous models where the stimulus is solely driven by strain energy (see, e.g., [34]). In contrast, in the

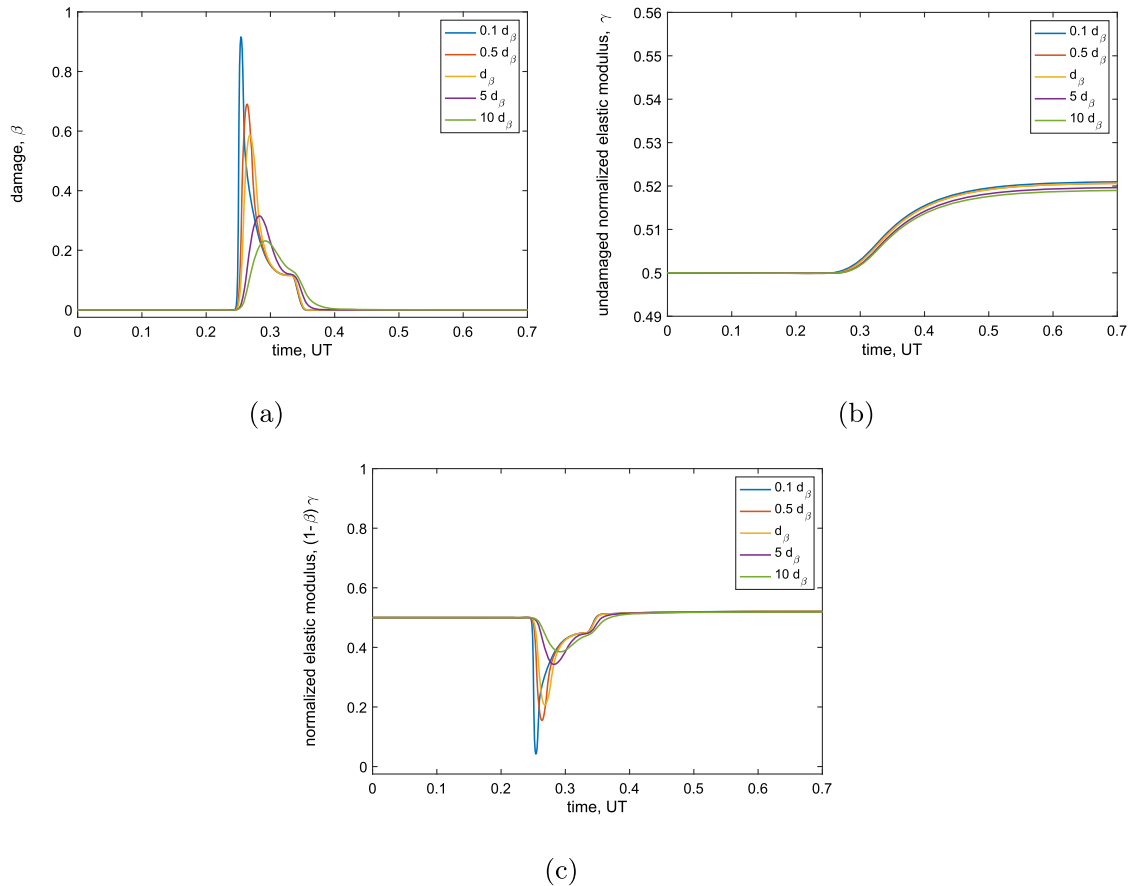


Fig. 5 Effect of the parameter d_β on damage (a), undamaged normalized elastic modulus (b), and normalized elastic modulus (c)

new proposed model, the presence of damage evolution introduces this crucial behavior. This behavior needs further investigation, but the introduction of damage seems essential from the preliminary results obtained for a more accurate representation of the bone remodeling process. Previously, the attempts made in the literature to obtain these responses were to introduce dissipation as a source triggering the stimulus [34,44,51] or by changing the dynamics of the stimulus with governing equations of a different nature than the diffusive one [40]. Since the phenomenon of bone remodeling is complex, we can expect all these aspects to coexist. Still, with numerical analyses, we have the opportunity to consider them separately, have a deeper understanding of each factor, and, thus, refine the model to the point that it may be really effective in practical clinical trials.

Finally, an analysis was carried out by varying the amplitude of the sinusoidal forcing F_0 by decreasing it by one-third with respect to its reference value and doubling it. The results align with what can be expected from this type of test. In fact, what happens is simply an increase in the healing speed as the amplitude increases, as shown in Figs. 9, 12, and 13. Once again, the overall qualitative behavior is unchanged. It is important to note that the aforementioned result only holds true if one remains within the elastic range in choosing F_0 .

4 Comparison with the undamageable model

This section presents a comparison between the proposed model and a previous version for the bone remodeling process [26]. The primary distinction between these models is the incorporation of a novel feature in the proposed refined version, which accounts for the damage phenomenon. This addition significantly enhances the accuracy and predictive capabilities of the newly proposed model compared to the original version. The numerical analysis demonstrates how including damage considerations improves the ability of the model to predict complex details of the process, making it an essential enhancement for a wide range of applications.

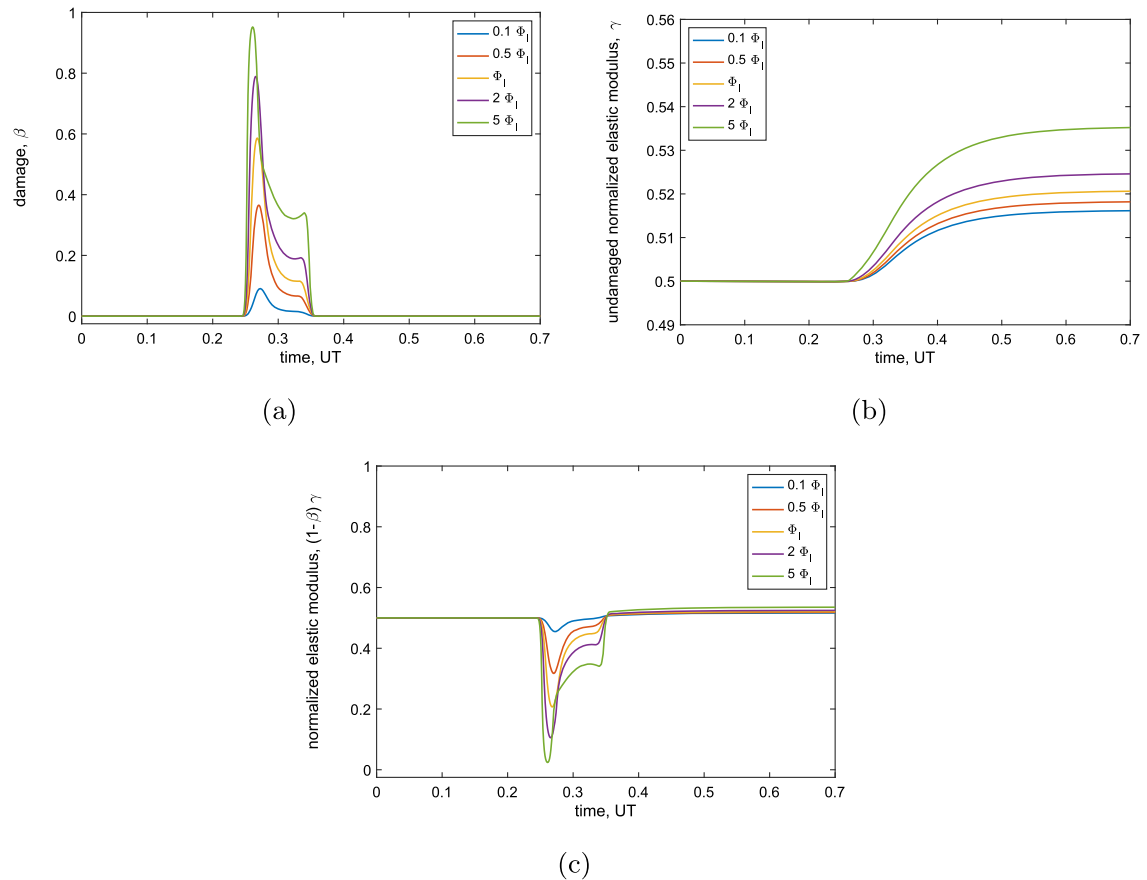


Fig. 6 Effect of the parameter Φ_ℓ on damage (a), undamaged normalized elastic modulus (b), and normalized elastic modulus (c)

Herein, the previous version of the model served as the baseline for comparison. It captures the fundamental characteristics of bone remodeling without accounting for damage. However, the newly developed model builds upon this foundation by introducing a damage consideration component, allowing it to factor in potential tissue deterioration and its effects on the process. In the absence of damage, the two considered models predict the same evolution of the bone tissue, given that, in the new version of the model, the only difference consists of adding the governing equations of the damage and its evolution. If the external force applied is small enough, the damage evolution is not triggered, and we revert to the previous scenario. Having chosen to evolve the elastic modulus γ instead of the apparent mass density here does not cause any changes. This is because, in the previous model, the two variables were linked by a bijective and monotonic phenomenological law. On the other hand, if the external forces are sufficiently high to cause some damage, their effect on the remodeling will be radically different.

Figure 14 illustrates the evolution of the comprehensive elastic modulus in the two models, without and with the accounting of the damage for a tensile test and a force sufficiently high to induce damage, namely, $F_0 = 64.29 \times 10^3$ N. The test carried out is the same as in Sect. 3.1. Clearly, in the case examined, it is impossible to neglect the effect of the damage because an essential aspect of the phenomenon would not be considered. Furthermore, the final value of the elastic modulus is also influenced by how the damage evolves, and depending on the case, this can lead to wrong and misleading predictions.

5 Conclusions

The paper is devoted to exploring one of the key factors that takes place in the bone remodeling process: the damage. Specifically, we considered a 1D continuous deformable body to describe the mechanical response

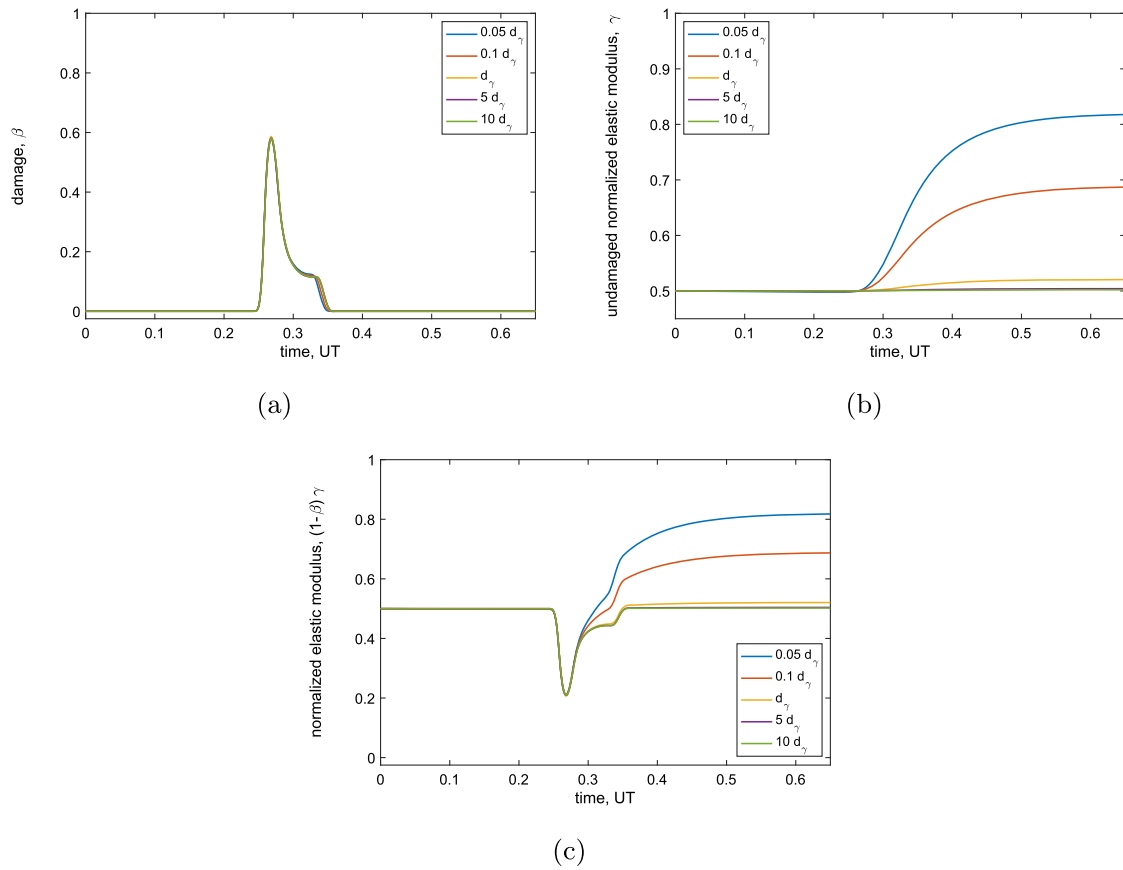


Fig. 7 Effect of the parameter d_γ on damage (a), undamaged normalized elastic modulus (b), and normalized elastic modulus (c)

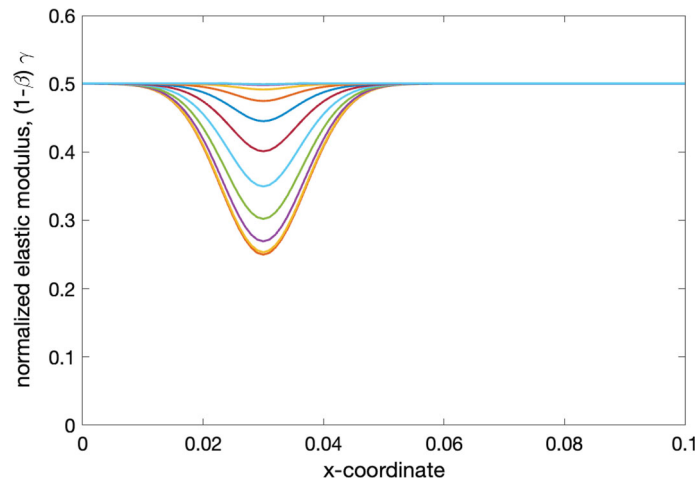


Fig. 8 Spatial evolution of the normalized elastic modulus at the point of maximum damage in the baseline case

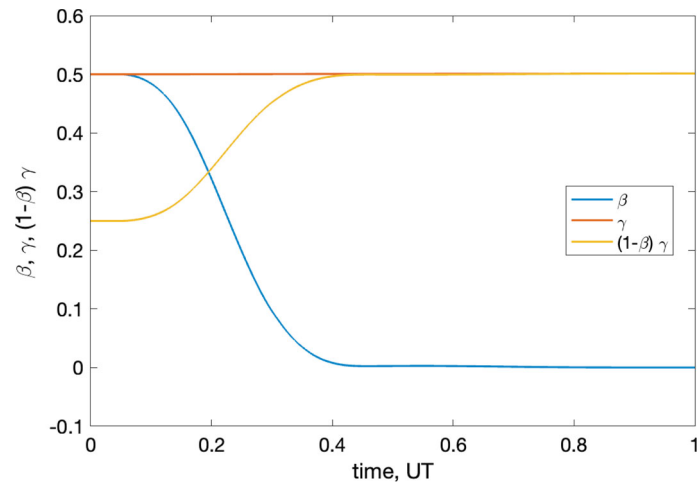


Fig. 9 Time evolution of damage and the undamaged and damaged elastic moduli for $f_h = 1 \text{ UT}^{-1}$

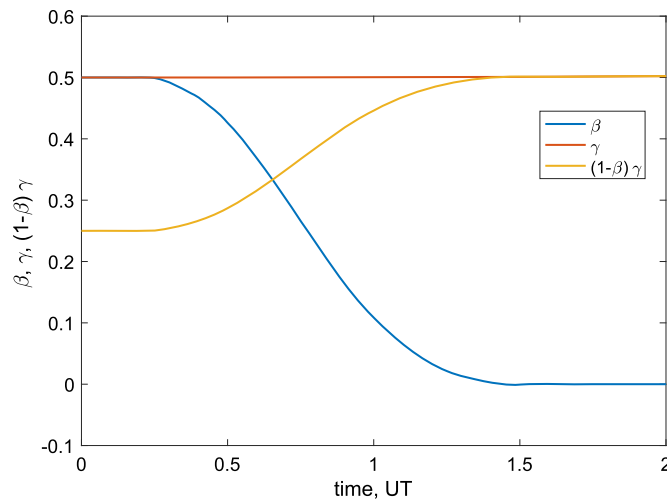


Fig. 10 Time evolution of damage and the undamaged and damaged elastic moduli for $f_h = 0.1 \text{ UT}^{-1}$

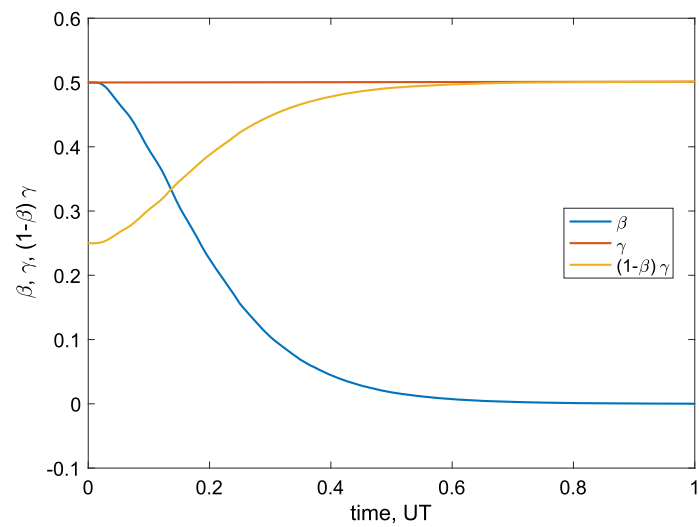


Fig. 11 Time evolution of damage and the undamaged and damaged elastic moduli for $f_h = 10 \text{ UT}^{-1}$

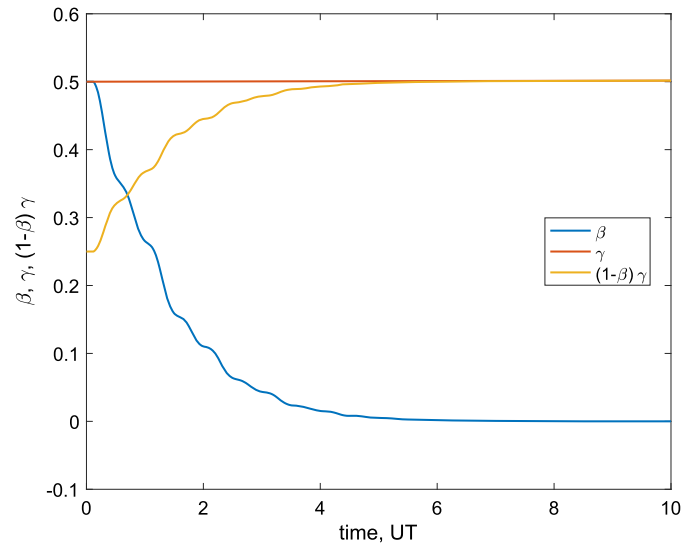


Fig. 12 Time evolution of damage and the undamaged and damaged elastic moduli for $F_0/3$

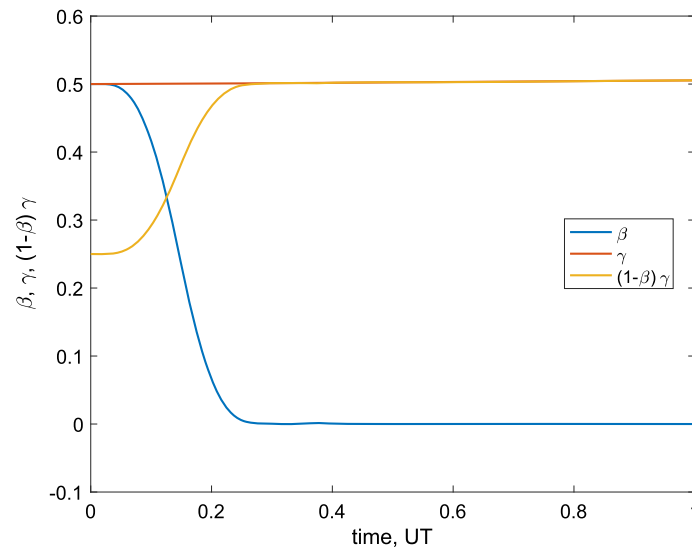


Fig. 13 Time evolution of damage and the undamaged and damaged elastic moduli for $2F_0$

of living bone tissue. The adaptive capability of the bone due to the remodeling process is incorporated in the model via an evolution law specified for an effective elastic modulus, γ , and based on a feedback mechanism guided by the mechanical response of the tissue. This information pertaining to the mechanical state is attributed to a signal of mechano-transduction that can spread into the tissue with diffusive behavior. This characteristic is essential since it is observed that in bone tissue, a remodeling process can occur even in regions where the signal cannot be produced for some injuries or pathologies. In this framework, we incorporate into the mechanical model the possibility that the tissue may be affected by damage and that this damage can evolve over time.

The purpose of the paper is twofold: 1) showcase the possible scenarios that this kind of model can predict and have a first look at its eligibility to be used in practical cases; 2) provide some theoretical guidelines to design experimental tests to corroborate its outcomes.

To these ends, we carried out several significant numerical simulations. A first set of numerical tests, where an external load has been set sufficiently high to induce damage, has been performed in order to analyze

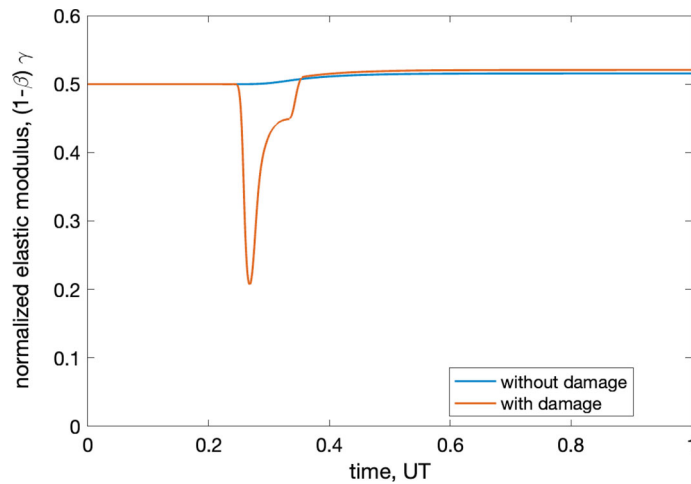


Fig. 14 Evolution of the normalized elastic modulus with and without damage

the evolution of the remodeling process. Subsequently, we have considered some initial damage and applied different cyclic loads with low magnitude to induce healing.

For the dynamic loading-induced damage case, we visualize the outcomes of the bone remodeling process through the elastic moduli involved, identify the damage evolution, and predict the extent of bone remodeling required for recovery. In the cyclic loading-induced healing case, we observe the evolution of bone tissue properties over multiple loading cycles and analyze the healing rate in relation to the loading frequency and amplitude.

The parametric numerical study, conducted using COMSOL Multiphysics, provides valuable insights into the bone remodeling process under dynamic and cyclic loading scenarios. The ability of the model to predict damage accumulation and healing rates showcases its potential for informing clinical decisions and implant designs related to bone health and repair.

By systematically exploring these two cases and their variations, we contribute to a deeper understanding of bone remodeling phenomena and offer a foundation for future research aimed at improving treatments for bone-related disorders and optimizing implant designs.

Incorporating damage considerations into the bone remodeling process framework represents a significant advancement. The ability of the proposed model to predict the impact of damage on the bone remodeling process enhances accuracy and detail prediction, providing a valuable tool for decision-making across various clinical trials. This model demonstrates the importance of continuously refining analytical tools to comprehensively capture real-world complexities.

The microstructure of bone is quite complex and develops on different temporal and spatial scales. In the paper, we adopted a relatively simple mechanical model to try to isolate the effect of damage on the remodeling process. However, a more refined model must undoubtedly take into account this inherent complexity in the nature of bone. Indeed, as future developments, we plan to address this complexity with generalized continuum models that can be deduced from homogenization methods as outlined in [52–60]. With this in mind, a critical aspect to consider to improve our model is porosity [61–65], which is directly related to the biological processes of remodeling and signal transmission.

From an experimental point of view, the present model should be not only identified but also better calibrated. For example, Eq. (4) implies an optimal value for the adaptive value $\gamma = \gamma_{opt} = 0.5$. An experimental investigation could characterize the material with a different value of γ_{opt} [66–69].

In this regard, one of the objectives of the paper is to provide also a model that allows theory-driven experiments to be designed and guided by the specific theoretical framework or hypotheses considered. Therefore, in this approach, starting with a model or hypotheses about how certain variables or factors are related, it is possible then to design a specific set of experiments to test these relationships or hypotheses. The model, thus, provides the foundation for formulating research questions, selecting variables, and designing experimental conditions. The primary goal is to test specific hypotheses derived from the theory. The experiments are conceived in order to manipulate certain variables and measure their effects on other variables, with the aim of either confirming or refuting the predictions of the theory. Theory-driven experiments typically follow

a systematic approach to data collection, analysis, and interpretation by using established methodologies and statistical techniques to ensure the validity and reliability of the findings. Results are interpreted within the context of the underlying theory. Whether the results support or contradict the theory, they provide valuable insights into the phenomena under investigation and contribute to the advancement of scientific knowledge.

Finally, an important aspect to consider for model development is the interaction with possible implants or prostheses. The ability to produce via 3D printing materials featuring complex substructures and exceptional mechanical properties, namely, metamaterials (see, e.g., [30,70–77]), presents a promising opportunity to enhance medical procedures and therapies, ultimately benefiting patients' quality of life. The potential lack of details due to the limited dimension of the 1D domain, adopted here, will easily be mitigated with a two- or three-dimensional problem since the formulation applies to these refined cases without any lack of generality.

Open Access This article is licensed under a Creative Commons Attribution 4.0 International License, which permits use, sharing, adaptation, distribution and reproduction in any medium or format, as long as you give appropriate credit to the original author(s) and the source, provide a link to the Creative Commons licence, and indicate if changes were made. The images or other third party material in this article are included in the article's Creative Commons licence, unless indicated otherwise in a credit line to the material. If material is not included in the article's Creative Commons licence and your intended use is not permitted by statutory regulation or exceeds the permitted use, you will need to obtain permission directly from the copyright holder. To view a copy of this licence, visit <http://creativecommons.org/licenses/by/4.0/>.

Funding Open access funding provided by Università degli Studi dell'Aquila within the CRUI-CARE Agreement.

Declarations

Conflict of interest The authors declare that they have no Conflict of interest.

Ethics approval Not applicable.

References

- Giorgio, I., dell'Isola, F., Andreaus, U., Misra, A.: An orthotropic continuum model with substructure evolution for describing bone remodeling: an interpretation of the primary mechanism behind Wolff's law. *Biomech. Model. Mechanobiol.* **22**(6), 2135–2152 (2023)
- Nowak, M.: On some properties of bone functional adaptation phenomenon useful in mechanical design. *Acta Bioeng. Biomech.* **12**(2), 49–54 (2010)
- Nowak, M.: New aspects of the trabecular bone remodeling regulatory model-two postulates based on shape optimization studies. *Dev. Novel Approach. Biomech. Metamater.* (2020). https://doi.org/10.1007/978-3-030-50464-9_6
- Hambli, R.: Micro-CT finite element model and experimental validation of trabecular bone damage and fracture. *Bone* **56**(2), 363–374 (2013)
- Hambli, R., Soulat, D., Gasser, A., Benhamou, C.-L.: Strain-damage coupled algorithm for cancellous bone mechano-regulation with spatial function influence. *Comput. Methods Appl. Mech. Eng.* **198**(33–36), 2673–2682 (2009)
- Garcia-Aznar, J.M., Rüberg, T., Doblare, M.: A bone remodelling model coupling microdamage growth and repair by 3D BMU-activity. *Biomech. Model. Mechanobiol.* **4**(2–3), 147–167 (2005)
- Hambli, R.: Connecting mechanics and bone cell activities in the bone remodeling process: an integrated finite element modeling. *Front. Bioeng. Biotechnol.* **2**, 6 (2014)
- Prendergast, P.J., Taylor, D.: Prediction of bone adaptation using damage accumulation. *J. Biomech.* **27**(8), 1067–1076 (1994)
- Addessi, D., Marfia, S., Sacco, E.: A plastic nonlocal damage model. *Comput. Methods Appl. Mech. Eng.* **191**(13–14), 1291–1310 (2002)
- Addessi, D.: A 2D Cosserat finite element based on a damage-plastic model for brittle materials. *Comput. Struct.* **135**, 20–31 (2014)
- Placidi, L., Misra, A., Barchiesi, E.: Simulation results for damage with evolving microstructure and growing strain gradient moduli. *Continuum Mech. Thermodyn.* **31**, 1143–1163 (2019)
- Abali, B.E., Klunker, A., Barchiesi, E., Placidi, L.: A novel phase-field approach to brittle damage mechanics of gradient metamaterials combining action formalism and history variable. *ZAMM-Zeitschrift für Angewandte Mathematik und Mechanik* **101**(9), 202000289 (2021)
- Bilotta, A., Morassi, A., Turco, E.: The use of quasi-isospectral operators for damage detection in rods. *Meccanica* **53**, 319–345 (2018)
- Fabbrocino, F., Funari, M.F., Greco, F., Lonetti, P., Luciano, R., Penna, R.: Dynamic crack growth based on moving mesh method. *Compos. B Eng.* **174**, 107053 (2019)
- Sessa, S., Barchiesi, E., Placidi, L., Paradiso, M., Turco, E., Hamila, N.: An insight into computational challenges in damage mechanics: analysis of a softening Hooke's spring. In: *Theoretical analyses, computations, and experiments of multiscale materials: a tribute to Francesco dell'Isola*, pp. 537–564. Springer, Cham (2022)

16. Vasiliev, V., Lurie, S., Solyaev, Y.: New approach to failure of pre-cracked brittle materials based on regularized solutions of strain gradient elasticity. *Eng. Fract. Mech.* **258**, 108080 (2021)
17. Gatta, C., Addessi, D.: Orthotropic multisurface model with damage for macromechanical analysis of masonry structures. *Eur. J. Mech.-A/Solids* **102**, 105077 (2023)
18. Bednarczyk, E., Lekszycki, T.: A novel mathematical model for growth of capillaries and nutrient supply with application to prediction of osteophyte onset. *ZAMP-Z. fur Angew. Math. Phys.* **67**(4), 1–14 (2016)
19. Bednarczyk, E., Lekszycki, T.: Evolution of bone tissue based on angiogenesis as a crucial factor: new mathematical attempt. *Math. Mech. Solids* **27**(6), 976–988 (2022)
20. Bersani, A.M., Dell’Acqua, G.: Asymptotic expansions in enzyme reactions with high enzyme concentrations. *Math. Methods Appl. Sci.* **34**(16), 1954–1960 (2011)
21. Burger, E.H., Klein-Nulend, J.: Mechanotransduction in bone-role of the lacunocanalicular network. *FASEB J.* **13**(9001), 101–112 (1999)
22. Mullender, M.G., Huiskes, R.: Proposal for the regulatory mechanism of Wolff’s law. *J. Orthop. Res.* **13**(4), 503–512 (1995)
23. Lekszycki, T., dell’Isola, F.: A mixture model with evolving mass densities for describing synthesis and resorption phenomena in bones reconstructed with bio-resorbable materials. *ZAMM-Z. Angew. Math. Mech.* **92**(6), 426–444 (2012)
24. George, D., Allena, R., Remond, Y.: A multiphysics stimulus for continuum mechanics bone remodeling. *Math. Mech. Complex Syst.* **6**(4), 307–319 (2018)
25. George, D., Allena, R., Remond, Y.: Integrating molecular and cellular kinetics into a coupled continuum mechanobiological stimulus for bone reconstruction. *Continuum Mech. Thermodyn.* **31**, 725–740 (2019)
26. Giorgio, I., dell’Isola, F., Andreaus, U., Alzahrani, F., Hayat, T., Lekszycki, T.: On mechanically driven biological stimulus for bone remodeling as a diffusive phenomenon. *Biomech. Model. Mechanobiol.* **18**(6), 1639–1663 (2019)
27. Pastrama, M.-I., Scheiner, S., Pivonka, P., Hellmich, C.: A mathematical multiscale model of bone remodeling, accounting for pore space-specific mechanosensation. *Bone* **107**, 208–221 (2018)
28. George, D., Allena, R., Remond, Y.: Integrating molecular and cellular kinetics into a coupled continuum mechanobiological stimulus for bone reconstruction. *Continuum Mech. Thermodyn.* **31**, 725–740 (2019)
29. Ciallella, A., Pulvirenti, M., Simonella, S.: Inhomogeneities in Boltzmann-SIR models. *Math. Mech. Complex Syst.* **9**, 273–292 (2021)
30. Giorgio, I., Spagnuolo, M., Andreaus, U., Scerrato, D., Bersani, A.M.: In-depth gaze at the astonishing mechanical behavior of bone: a review for designing bio-inspired hierarchical metamaterials. *Math. Mech. Solids* **26**(7), 1074–1103 (2021)
31. Hellmich, C., Kober, C., Erdmann, B.: Micromechanics-based conversion of CT data into anisotropic elasticity tensors, applied to FE simulations of a mandible. *Ann. Biomed. Eng.* **36**, 108–122 (2008)
32. Hellmich, C., Ukaj, N., Smeets, B., Van Oosterwyck, H., Filipovic, N., Zelaya-Lainez, L., Kalliauer, J., Scheiner, S.: Hierarchical biomechanics: concepts, bone as prominent example, and perspectives beyond. *Appl. Mech. Rev.* **74**(3), 030802 (2022)
33. Beaupré, G., Orr, T., Carter, D.: An approach for time-dependent bone modeling and remodeling-theoretical development. *J. Orthop. Res.* **8**(5), 651–661 (1990)
34. Giorgio, I., Andreaus, U., Scerrato, D., dell’Isola, F.: A visco-poroelastic model of functional adaptation in bones reconstructed with bio-resorbable materials. *Biomech. Model. Mechanobiol.* **15**(5), 1325–1343 (2016)
35. McNamara, L.M., Prendergast, P.J.: Bone remodelling algorithms incorporating both strain and microdamage stimuli. *J. Biomech.* **40**(6), 1381–1391 (2007)
36. Klein-Nulend, J., Van Der Plas, A., Semeins, C.M., Ajubi, N.E., Erangos, J.A., Nijweide, P.J., Burger, E.H.: Sensitivity of osteocytes to biomechanical stress in vitro. *FASEB J.* **9**(5), 441–445 (1995)
37. Scheiner, S., Pivonka, P., Hellmich, C.: Poromicromechanics reveals that physiological bone strains induce osteocyte-stimulating lacunar pressure. *Biomech. Model. Mechanobiol.* **15**, 9–28 (2016)
38. Scheiner, S., Pivonka, P., Hellmich, C.: Coupling systems biology with multiscale mechanics, for computer simulations of bone remodeling. *Comput. Methods Appl. Mech. Eng.* **254**, 181–196 (2013)
39. Colloca, M., Blanchard, R., Hellmich, C., Ito, K., Rietbergen, B.: A multiscale analytical approach for bone remodeling simulations: linking scales from collagen to trabeculae. *Bone* **64**, 303–313 (2014)
40. Scerrato, D., Giorgio, I., Bersani, A.M., Andreucci, D.: A proposal for a novel formulation based on the hyperbolic Cattaneo’s equation to describe the mechano-transduction process occurring in bone remodeling. *Symmetry* **14**(11), 2436 (2022)
41. Mavčič, B., Antolič, V.: Optimal mechanical environment of the healing bone fracture/osteotomy. *Int. Orthop.* **36**, 689–695 (2012)
42. Eriksen, E.F.: Cellular mechanisms of bone remodeling. *Rev. Endocr. Metab. Disord.* **11**(4), 219–227 (2010)
43. Bartl, R., Bartl, C., Bartl, R., Bartl, C.: Modelling and remodelling of bone. *Bone disorders: biology, diagnosis, prevention, therapy*, 21–30 (2017)
44. Huiskes, R.: If bone is the answer, then what is the question? *J. Anat.* **197**(2), 145–156 (2000)
45. Qin, Q.-H., Wang, Y.-N.: A mathematical model of cortical bone remodeling at cellular level under mechanical stimulus. *Acta Mech. Sin.* **28**, 1678–1692 (2012)
46. Lanyon, L.: Functional strain in bone tissue as an objective, and controlling stimulus for adaptive bone remodelling. *J. Biomech.* **20**(11–12), 1083–1093 (1987)
47. Thompson, W.R., Yen, S.S., Rubin, J.: Vibration therapy: clinical applications in bone. *Curr. Opin. Endocrinol. Diabetes Obes.* **21**(6), 447 (2014)
48. Lambers, F.M., Koch, K., Kuhn, G., Ruffoni, D., Weigt, C., Schulte, F.A., Müller, R.: Trabecular bone adapts to long-term cyclic loading by increasing stiffness and normalization of dynamic morphometric rates. *Bone* **55**(2), 325–334 (2013)
49. Ehrlich, P.J., Lanyon, L.E.: Mechanical strain and bone cell function: a review. *Osteoporos. Int.* **13**(9), 688 (2002)
50. Lanyon, L.E., Rubin, C.: Static vs dynamic loads as an influence on bone remodelling. *J. Biomech.* **17**(12), 897–905 (1984)
51. Kumar, C., Jasiuk, I., Dantzig, J.: Dissipation energy as a stimulus for cortical bone adaptation. *J. Mech. Mater. Struct.* **6**(1), 303–319 (2011)

52. Abali, B.E., Barchiesi, E.: Additive manufacturing introduced substructure and computational determination of metamaterials parameters by means of the asymptotic homogenization. *Continuum Mech. Thermodyn.* **33**(4), 993–1009 (2021)
53. Yang, H., Abali, B.E., Müller, W.H., Barboura, S., Li, J.: Verification of asymptotic homogenization method developed for periodic architected materials in strain gradient continuum. *Int. J. Solids Struct.* **238**, 111386 (2022)
54. Jakabčič, L., Seppacher, P.: On periodic homogenization of highly contrasted elastic structures. *J. Mech. Phys. Solids* **144**, 104104 (2020)
55. Barchiesi, E., dell’Isola, F., Hild, F., Seppacher, P.: Two-dimensional continua capable of large elastic extension in two independent directions: asymptotic homogenization, numerical simulations and experimental evidence. *Mech. Res. Commun.* **103**, 103466 (2020)
56. Cuomo, M., Boutin, C., Contrafatto, L., Gazzo, S.: Effective anisotropic properties of fibre network sheets. *Eur. J. Mech.-A/Solids* **93**, 104492 (2022)
57. Gazzo, S., Cuomo, M., Boutin, C., Contrafatto, L.: Directional properties of fibre network materials evaluated by means of discrete homogenization. *Eur. J. Mech.-A/Solids* **82**, 104009 (2020)
58. Falsone, G., La Valle, G.: A homogenized theory for functionally graded Euler-Bernoulli and Timoshenko beams. *Acta Mech.* **230**, 3511–3523 (2019)
59. Spagnuolo, M., Yildizdag, M.E., Andreaus, U., Cazzani, A.M.: Are higher-gradient models also capable of predicting mechanical behavior in the case of wide-knit pantographic structures? *Math. Mech. Solids* **26**(1), 18–29 (2021)
60. Tepedino, M.: The mechanical role of the periodontal ligament for developing mathematical models in orthodontics. *Math. Mech. Complex Syst.* **11**(4), 525–539 (2023)
61. Grillo, A., Logashenko, D., Stichel, S., Wittum, G.: Simulation of density-driven flow in fractured porous media. *Adv. Water Resour.* **33**(12), 1494–1507 (2010)
62. Penta, R., Miller, L., Grillo, A., Ramírez-Torres, A., Mascheroni, P., Rodríguez-Ramos, R.: Porosity and diffusion in biological tissues Recent advances and further perspectives. *Const. Modell. Solid Contin.* (2020). https://doi.org/10.1007/978-3-030-31547-4_11
63. De Cicco, S., Ieşan, D.: On the theory of thermoelastic materials with a double porosity structure. *J. Therm. Stresses* **44**(12), 1514–1533 (2021)
64. De Cicco, S., De Angelis, F.: A plane strain problem in the theory of elastic materials with voids. *Math. Mech. Solids* **25**(1), 46–59 (2020)
65. Eremeyev, V.A., Skrzat, A., Stachowicz, F., Vinakurava, A.: On strength analysis of highly porous materials within the framework of the micropolar elasticity. *Proc. Struct. Integr.* **5**, 446–451 (2017)
66. Placidi, L., Andreaus, U., Della Corte, A., Lekszycki, T.: Gedanken experiments for the determination of two-dimensional linear second gradient elasticity coefficients. *Z. Angew. Math. Phys.* **66**(6), 3699–3725 (2015). <https://doi.org/10.1007/s00033-015-0588-9>
67. De Angelo, M., Yılmaz, N., Yildizdag, M.E., Misra, A., Hild, F., Dell’isola, F.: Identification and validation of constitutive parameters of a hencky-type discrete model via experiments on millimetric pantographic unit cells. *Int. J. Non-Linear Mech.* **153**, 104419 (2023)
68. Cefis, N., Fedele, R., Beghi, M.G.: An integrated methodology to estimate the effective elastic parameters of amorphous TiO₂ nanostructured films, combining SEM images, finite element simulations and homogenization techniques. *Mech. Res. Commun.* **131**, 104153 (2023)
69. Fedele, R., Maier, G., Miller, B.: Identification of elastic stiffness and local stresses in concrete dams by in situ tests and neural networks. *Struct. Infrastruct. Eng.* **1**(3), 165–180 (2005)
70. Eremeyev, V., Skrzat, A., Vinakurava, A.: Application of the micropolar theory to the strength analysis of bioceramic materials for bone reconstruction. *Strength Mater.* **48**, 573–582 (2016)
71. dell’Isola, F., Seppacher, P., Alibert, J.J., et al.: Pantographic metamaterials: an example of mathematically driven design and of its technological challenges. *Continuum Mech. Thermodyn.* **31**, 851–884 (2019)
72. Carcaterra, A., dell’Isola, F., Esposito, R., Pulvirenti, M.: Macroscopic description of microscopically strongly inhomogeneous systems: A mathematical basis for the synthesis of higher gradients metamaterials. *Arch. Ration. Mech. Anal.* **218**, 1239–1262 (2015)
73. dell’Isola, F., Misra, A.: Principle of virtual work as foundational framework for metamaterial discovery and rational design. *Comptes Rendus. Mécanique* **351**(S3), 1–25 (2023)
74. dell’Isola, F., Lekszycki, T., Pawlikowski, M., Grygoruk, R., Greco, L.: Designing a light fabric metamaterial being highly macroscopically tough under directional extension: first experimental evidence. *Z. Angew. Math. Phys.* **66**, 3473–3498 (2015)
75. Eremeyev, V.A., Turco, E.: Enriched buckling for beam-lattice metamaterials. *Mech. Res. Commun.* **103**, 103458 (2020)
76. Solyaev, Y., Lurie, S., Altenbach, H., dell’Isola, F.: On the elastic wedge problem within simplified and incomplete strain gradient elasticity theories. *Int. J. Solids Struct.* **239**, 111433 (2022)
77. Mancusi, G., Fabbrocino, F., Feo, L., Fraternali, F.: Size effect and dynamic properties of 2d lattice materials. *Compos. B Eng.* **112**, 235–242 (2017)